Proc. Natl. Acad. Sci. USA
Vol. 95, pp. 12141–12146, October 1998
Biochemistry

Oligomerization domain-directed reassembly of active dihydrofolate reductase from rationally designed fragments

JOELLE N. PELLETIER, F.-X. CAMPBELL-VALOIS, AND STEPHEN W. MICHNICK*

Département de biochimie, Université de Montréal, Montréal, QC H3T 1J4, Canada

Edited by Gregory A. Petsko, Brandeis University, Waltham, MA, and approved August 20, 1998 (received for review June 10, 1998)

ABSTRACT **Reassembly of enzymes from peptide fragments has been used as a strategy for understanding the evolution, folding, and role of individual subdomains in catalysis and regulation of activity. We demonstrate an oligomerization-assisted enzyme reassembly strategy whereby fragments are covalently linked to independently folding and interacting domains whose interactions serve to promote efficient refolding and complementation of fragments, forming active enzyme. We show that active murine dihydrofolate reductase (E.C. 1.5.1.3) can be reassembled from complementary N- and C-terminal fragments when fused to homodimerizing GCN4 leucine zipper-forming sequences as well as heterodimerizing protein partners. Reassembly is detected by an *in vivo* selection assay in *Escherichia coli* and *in vitro*. The effects of mutations that disrupt fragment affinity or enzyme activity were assessed. The steady–state kinetic parameters for the reassembled mutant (Phe-31 → Ser) were determined; they are not significantly different from the full-length mutant. The strategy described here provides a general approach for protein dissection and domain swapping studies, with the capacity both for rapid *in vivo* screening as well as *in vitro* characterization. Further, the strategy suggests a simple *in vivo* enzyme-based detection system for protein–protein interactions, which we illustrate with two examples: ras–GTPase and raf–ras-binding domain and FK506-binding protein-rapamycin complexed with the target of rapamycin TOR2.**

Protein fragment complementation studies have been used to address a number of important questions including gene structure (1), the role of primary sequence in determining the tertiary structure of proteins (2), protein folding (3, 4), and the role of tertiary structure elements in enzyme catalysis (5) to probe macromolecular assembly (6) and to test theories of protein evolution (7). Novel applications of fragment complementation also have been suggested, including the use of protein fragments in dominant selection studies (8). Recently, we and others (9–12) have illustrated that protein (or enzyme) fragment complementation can be used in the *in vivo* detection of protein–protein interactions.

The detection of activity of enzymes reassembled from fragments is usually frustrated by insolubility of fragments and/or inefficient reassembly of the fragments into native structure. We propose a strategy for the directed, noncovalent association of enzyme fragments, combined with *in vivo* detection of the activity: First, addition of soluble oligomerization domains to the fragments to favor their folding and assembly, via soluble linkers to allow optimal orientation for assembly. Second, an *in vivo*-screening assay for fragment complexation, in which lower levels of activity are needed than for detection by *in vitro* assays. By reconstituting enzymatic activity in a noncovalent assembly, we will have at hand a tool for answering the following questions: Do the noncovalently associated fragments allow formation of the active fold? Do the reassociated fragments allow native-like activity, with kinetics that are similar to the full-length enzyme? What effect does disruption of the sequence have on the folding and activity? And finally, can the rigidity imposed by the native covalent linkage between the fragments be replaced by the flexibility of noncovalently interacting peptides?

Here, we describe the oligomerization-assisted complementation of fragments of murine dihydrofolate reductase (mDHFR) (E.C. 1.5.1.3) as an example of dissecting an enzyme into fragments and functional reassembly of those fragments into active enzyme. DHFR has been described as comprising three structural fragments forming two domains: the adenine-binding domain (fragment 2, or F[2]) and a discontinuous domain (F[1] and F[3]) (13, 14). The folate-binding pocket and the NADPH-binding groove are formed mainly by residues belonging to F[1] and F[2]. Only 4 of 29 residues that make contacts with the substrates belong to F[3] (15), and none of these residues is directly implicated in catalysis.

Folding of fragments of *Escherichia coli* DHFR has revealed that only certain fragments, alone or in combination, adopt substantial secondary and tertiary structure (13). However, circular permutation of *E. coli* as well as mDHFR has shown that its primary structure can be radically altered and yet yield active enzyme with native-like structure (16). We have designed two fragments of mDHFR consisting of the sequences coding for F[1,2], and for F[3], each of which is covalently linked to an interacting domain (GCN4 leucine zipper). We demonstrate the leucine zipper-dependent reassembly of catalytically active mDHFR from its fragments and examine the effects of fragment interface mutations and of active site mutations on fragment complementation. Finally, we demonstrate detection of two known protein–protein interactions *in vivo*, those of p21 ras GTPase with its target the *ras*-binding domain (RBD) of the Ser/Thr kinase *raf* and the rapamycin-mediated interaction of the immunophillin FKBP with the *Saccharomyces cerevisiae* yeast target of rapamycin (TOR2).

The strategy described here could provide a valuable tool in understanding the contribution of functional motifs to enzymatic activity and in the definition of functional building blocks that can be rationally assembled in the design of new protein catalysts. This binary association strategy ensures that the building blocks will always be brought together, regardless of their structure, in a directed and productive manner. Finally, we discuss the use of this strategy for cDNA library screening to identify protein–protein interactions or in directed evolution of proteins.

The publication costs of this article were defrayed in part by page charge payment. This article must therefore be hereby marked "*advertisement*" in accordance with 18 U.S.C. §1734 solely to indicate this fact.

This paper was submitted directly (Track II) to the *Proceedings* office.

Abbreviations: PCA, protein fragment complementation assay; F, fragment, F[1,2], F[3]; mDHFR, murine dihydrofolate reductase; hDHFR, human DHFR; Z-F[1,2], GCN4 leucine zipper-mDHFR fragment[1,2]; IPTG, isopropyl-β-D-thiogalactopyranoside; FKBP, FK506-binding protein; TOR2, target of rapamycin; MTX, methotrexate; RBD, *ras–raf* binding domain of *raf*.

*To whom reprint requests should be addressed. e-mail: michnick@bch.umontreal.ca.

MATERIALS AND METHODS

Materials. All reagents used were of the highest available purity. Mutagenic and sequencing oligonucleotides were purchased from GIBCO/BRL. Restriction endonucleases and DNA-modifying enzymes were from Pharmacia and New England Biolabs. *E. coli* strains DH5α and GM2163 (dcm$^-$; New England Biolabs) were used for subcloning. For protein overexpression, *E. coli* strain BL21 carrying plasmid pRep4 (Qiagen, *lac* I^q) was transformed with the appropriate DNA constructs.

DNA Constructs. We constructed vectors allowing the expression of mDHFR fragments covalently linked to a hexahistidine peptide (Qiagen pQE series) and a leucine zipper (Fig. 1). The full-length mDHFR is expressed from pQE-16. mDHFR fragments carrying their own in-frame stop codon were subcloned into pQE-32, downstream from and in-frame with the GCN4 leucine zipper-coding sequence. All final constructs were verified by DNA sequencing.

Expression Vectors Harboring the Oligomerization Domains. Residues 235–281 of the GCN4 leucine zipper (a *Sal*I–*Bam*HI (blunted) 254-bp fragment) were obtained from pRS316 harboring that sequence (10). The fragment was ligated to pQE-32 linearized with *Sal*I–*Hin*dIII (blunted). The product, construct Z, codes for: Met-Arg-Gly-Ser followed by a hexahistidine tag and 13 residues preceding the 47 GCN4 leucine zipper residues. RBD of raf were obtained by PCR amplification of pTcras and pDW333, respectively. TOR2 rapamycin-binding domain and FKBP were amplified by PCR from pMRS315 and pNH1, respectively. They were cloned respectively by *Xma*I–*Nhe*I and *Sph*I–*Nhe*I in pQE32.

Creation of DHFR Fragments. The eukaryotic expression vector pMT3 harboring the mDHFR-coding sequence (17) was used as a template for PCR-generation of mDHFR containing the features allowing subcloning and separate expression of F[1,2] and F[3] (Fig. 1). A *Bsp*EI site at either terminus of the coding sequence, a stop codon after F[1,2], followed by a *Spe*I site for use in subcloning F[3], were created by PCR.

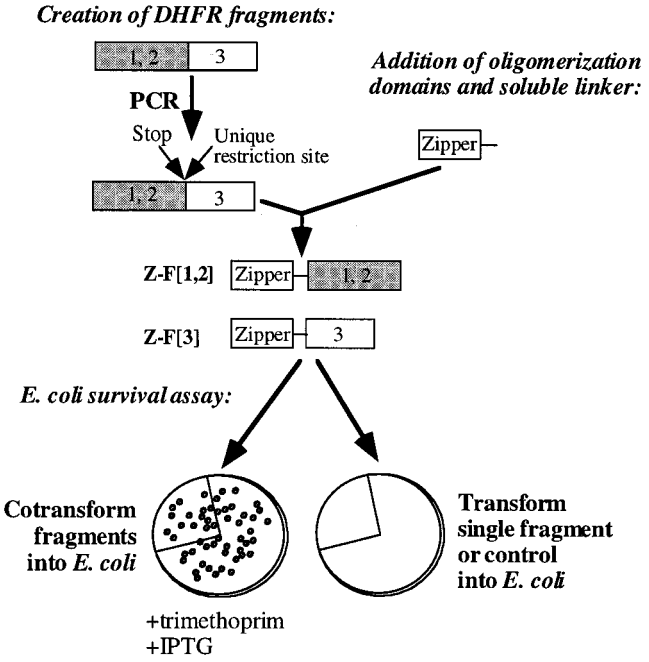

FIG. 1. Scheme of mDHFR fragmentation and of the DHFR fragment complementation assay. The homodimerizing GCN4 leucine zipper (Zipper), and mDHFR fragments (1, 2, and 3) are illustrated. The labels for the constructs are used to identify both the DNA constructs and the proteins expressed from these constructs.

Construction of a Flexible Linker and Subcloning of F[1,2] and F[3]. Complementary oligonucleotides containing the restriction sites: *Sna*BI, *Nhe*I, *Spe*I, and *Bsp*EI and coding for a flexible linker were hybridized together and inserted into pMT3 at a unique *Eco*RI site. The PCR product (described above) was inserted at *Bsp*EI, yielding construct [1,2,3]. The 610-bp *Bsp*EI–*Eco*NI fragment of construct [1,2,3] coding for F[1,2] was subcloned into pMT3, yielding construct F[1,2]. The 250-bp *Spe*I–*Bsp*EI fragment of construct [1,2,3] coding for DHFR F[3] was subcloned into pMT3 yielding construct F[3].

Creation of the Expression Constructs. Fragments of constructs F[1,2] or F[3] coding for the DHFR fragments, were subcloned into construct Z, downstream from the zipper-coding sequence. The resulting constructs, Z-F[1,2] and Z-F[3], code for the zipper, followed by an 11 residue flexible linker and mDHFR F[1,2] or F[3], respectively (Figs. 1 and 2*A*). The fragment coding for the GCN4 zipper was removed

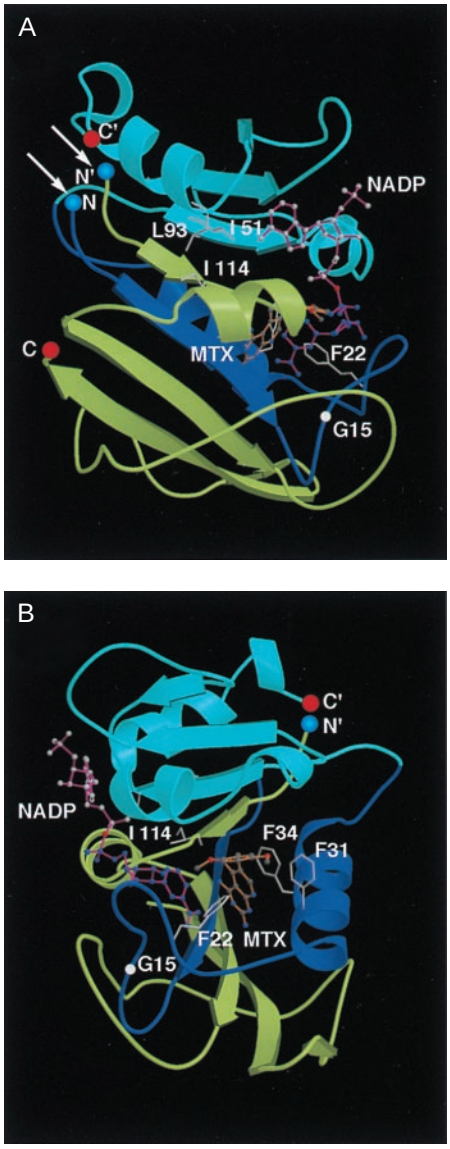

FIG. 2. Structure of hDHFR (32) showing fragments F[1,2] (blue-cyan) and F[3] (yellow) bound NADPH (violet) and methotrexate-γ-tetrazole (gold). (*A*) Natural and fragment N and C termini (N, C, and N′, C′, respectively) are indicated by blue or red circles. Arrows indicate location of fusion to oligomerizing proteins. Position of Ile-114 and contact residues in F[1,2] (Ile-51 and Leu-93) are indicated. (*B*) Ninety degree vertical axis rotation of view in *A* showing positions of methotrexate resistance mutations.

from construct Z-F[1,2] by restriction yielding digestion and religation, construct control-F[1,2].

Creation of Mutants. Site-directed mutagenesis was performed on fragments of Z-F[1,2] or Z-F[3] subcloned into pBluescript SK^+ (Stratagene), using oligonucleotides that encode a silent mutation producing or destroying a diagnostic restriction site. Fragments of putative mutants identified by restriction were subcloned back into Z-F[1,2] or Z-F[3]. The mutations were confirmed by DNA sequencing.

***E. coli* Survival Assay.** Competent *E. coli* BL21/pRep4 were transformed with the appropriate constructs and washed twice with M9 minimal medium before plating on M9 Petris containing 50 μg/ml kanamycin, 100 μg/ml ampicillin, and 0.5 μg/ml trimethoprim. One-half of each transformation mixture was plated in the absence and the second half in the presence of 1 mM isopropyl-β-D-thiogalactopyranoside (IPTG). All plates were placed at 37°C for 66 hr. For the ras–raf and FKBP–TOR2 cotransformation, 80 μM thymine was added to the medium. The optimal results for the FKBP-TOR2 experiments were obtained with minimal medium plates containing 1 μM rapamycin (Calbiochem) and incubation at 30°C.

***E. coli* Growth Curves.** Growth rates were determined in liquid Ma medium supplemented with ampicillin, kanamycin as well as IPTG (1 mM), and trimethoprim (1 μg/ml) where indicated. Because cells cotransformed with constructs Z-F[1,2] + Z-F[3:Ile-114 → Gly] did not form colonies when plated under selective pressure, double transformants were obtained under nonselective conditions (+kanamycin and ampicillin) and screening for the presence of the two constructs by restriction analysis. All experiments were performed in triplicate. Aliquots were withdrawn periodically for measurement of optical density. Doubling time was calculated for early logarithmic growth (OD_{600} between 0.02 and 0.2).

Protein Overexpression and Purification. Bacteria were propagated in medium or in Terrific Broth in the presence of the appropriate antibiotics to an OD_{600} of ≈1.0. Expression was induced by addition of 1 mM IPTG and further incubation for 24 hr if in minimal medium or 3 hr if in Terrific Broth. Small-scale denaturing and large-scale native purifications were performed on Ni-NTA agarose (Qiagen) according to the manufacturer's protocol. After native purification, imidazole was dialyzed out at 4°C against three changes of 300 vol of buffer A [100 mM potassium phosphate, pH 7.5/1 mM phenylmethylsulfonyl fluoride/1 mM β-mercaptoethanol]. As a control, untransformed cells were submitted to the same procedure for parallel enzymatic analysis.

Enzyme Assays. DHFR activity was monitored by fluorimetry, to follow tetrahydrofolate production (λ exc. = 310 nm; λ em. = 360 nm). Quenching of tetrahydrofolate by DHF and NADPH was corrected for, with a tetrahydrofolate standard curve. Concentrations of substrates were determined spectrophotometrically. The reaction buffer was freshly prepared buffer A containing 10 mM β-mercaptoethanol. Initial rates were measured under conditions in which <15% conversion to product had occurred. For determination of specific activity, the concentration of reconstituted enzyme was estimated by methotrexate (MTX) inhibition of the DHFR activity. For the MTX-resistant Phe-31 → Ser mutant, the concentration of enzyme present was in the range of K_i (MTX) and therefore could not be determined with high accuracy. Unless otherwise indicated, the concentration of NADPH was constant at 25 μM in determinations of K_m (DHF) and K_i (MTX). The range of MTX concentrations used in K_i determinations was 100 pM–30 nM. DHF concentrations of 5 μM, 10 μM, and 30 μM were used in Dixon representations for determination of K_i (MTX) and K_m (NADPH). In the indirect determination of K_m (NADPH), NADPH concentrations used were 10 μM, 25 μM, and 50 μM. All data were fitted to the Michealis–Menten equation by using the nonlinear regression analysis programs AXUM (Mathsoft, Cambridge, MA) and MACCURVE FIT (K. Raner Software, Mt. Waverley, Australia).

RESULTS

Design Considerations. mDHFR is a small (21 kDa), monomeric protein which shares high sequence identity with the human DHFR (hDHFR) sequence (91% identity) and is highly homologous to the *E. coli* enzyme (29% identity, 68% homology). Comparison of the crystal structures of mDHFR and hDHFR suggests that their active sites and substrate-binding pockets are identical and homologous to those of *E. coli* DHFR (15). The folate-binding pocket and the NADPH-binding groove are formed mainly by residues belonging to the adenine-binding domain (F[2]) and the N-terminal portion of the discontinuous domain (F[1]) (Fig. 2 *A* and *B*).

Residues 101–108 of hDHFR, at the junction between F[2] and F[3], form a disordered loop, which can be disrupted with no significant effect on activity (18). We chose to fragment mDHFR between F[1,2] and F[3], at residue 107, so as to cause minimal disruption of the active site and NADPH cofactor-binding sites. The native N terminus of mDHFR and the N terminus created by fragmentation occur on the same surface of the enzyme (Fig. 2*A*) (15) facilitating N-terminal fusion to the leucine zipper sequences and the other oligomerizing proteins used in this study.

***E. coli* Survival Assays.** *E. coli* DHFR is selectively inhibited by the anti-folate drug trimethoprim. Because mammalian DHFR has a 12,000-fold lower affinity for trimethoprim than does bacterial DHFR (19), growth of bacteria expressing mDHFR in the presence of trimethoprim levels lethal to bacteria is an efficient means of selecting for reassembly of mDHFR fragments into an active enzyme (Fig. 1). Fig. 3*A* illustrates the results of cotransformation of bacteria with constructs Z-F[1,2] and Z-F[3] in the presence of IPTG and trimethoprim, clearly showing that colony growth under selective pressure is possible only in cells expressing both fragments of mDHFR. There is no growth in cells expressing either Z-F[1,2] or Z-F[3] alone. Oligomerization domains on both fragments of mDHFR are essential as illustrated by cotransformation of bacteria with both vectors coding for mDHFR fragments, only one of which carries a leucine zipper (Fig. 3*A*) and by the fact that when noninteracting oligomerization domains are tested, no growth is observed (Fig. 4). The presence of both plasmids in bacteria grown in trimethoprim was confirmed by restriction analysis of the plasmids isolated from individual colonies and by detection of overexpression of proteins of the expected molecular weight on SDS/PAGE of the crude lysate from Terrific Broth (data not shown).

Affinity Mutants. We made point mutations at the interface between the DHFR fragments to test first, whether reconstitution of DHFR activity is due to specific reassembly of its fragments and second, whether subtle changes in the protein stability could be detected. It could be argued that the reconstitution we observed was due to nonspecific association of F[1,2] with F[3]; a reduction of observed activity in the *in vivo* assay by site-specific mutations directed at the interface would confirm that the reconstitution is due to native-like structural reassembly. Part of the interface belongs to the hydrophobic core of DHFR. Core mutations that sequentially reduce affinity of the two fragments for each other (20) should cause a sequential reduction of response in our assay. We generated mutants of F[3] at Ile-114, whose sidechain contacts residues in F[1,2] (Fig. 2*A*) and cotransformed *E. coli* with Z-F[1,2] and the mutated Z-F[3:Ile-114 → Val], Z-F[3:Ile-114 → Ala] or Z-F[3:Ile-114 → Gly] (Fig. 3*B*). The colonies containing Z-F[3:Ile-114 → Ala] grew significantly slower than those containing Z-F[3] or Z-F[3:Ile-114 → Val]. No growth was detected with Z-F[3:Ile-114 → Gly]. The number of transformants obtained was not significantly different in the cases in which colonies were observed, implying that cells

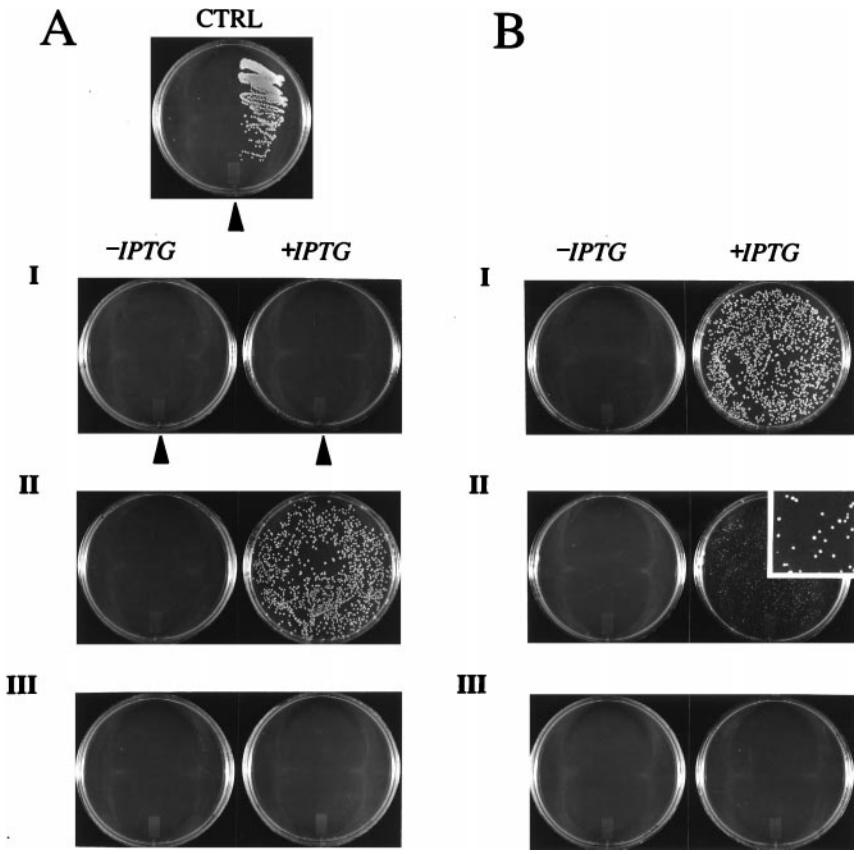

FIG. 3. (A) *E. coli* survival assay on minimal medium plates. Control, left side of the plate: *E. coli* harboring pQE-30 (no insert); right side: *E. coli* expressing full-length mDHFR. (*A*, I) Left half of each plate: transformation with Z-F[1,2]; right half of each plate: transformation with Z-F[3]. (*A*, II) Cotransformation with Z-F[1,2] and Z-F[3]. (*A*, III) Cotransformation with constructs control-F[1,2] and Z-F[3]. All plates contain 0.5 μg/ml trimethoprim and plates on the right side of I-III contain 1 mM IPTG. (*B*) *E. coli* survival assay using destabilizing DHFR mutants. (*B*, I) Cotransformation with Z-F[1,2] and Z-F[3:Ile-114 → Val]. (*B*, II) Cotransformation with Z-F[1,2] and Z-F[3:Ile-114 → Ala]. (*Inset*) A 5-fold enlargement of the right-side plate. (*B*, III) Cotransformation with Z-F[1,2] and Z-F[3:Ile-114 → Gly]. All plates contain 0.5 μg/ml trimethoprim and plates on the right side contain 1 mM IPTG.

cotransformed with Z-F[1,2] and either Z-F[3], Z-F[3:Ile-114 → Val], or Z-F[3:Ile-114 → Ala] have an equal survival rate.

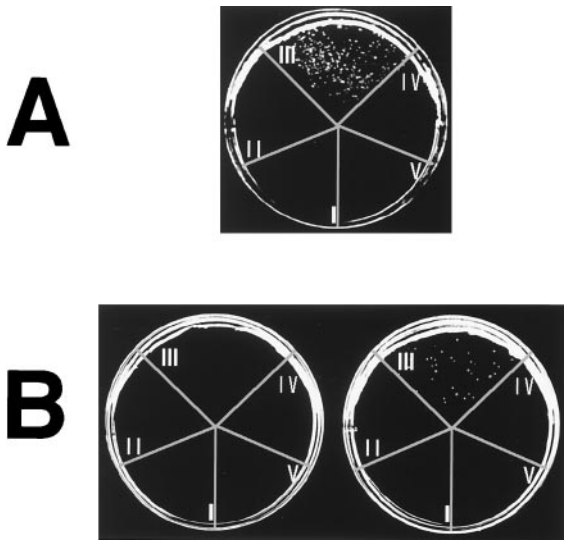

FIG. 4. *E. coli* survival assay as in Fig. 3 Ras and Raf (*A*). Cotransformation with raf-F[1,2] alone (I); ras-F[3] alone (II); raf-F[1,2] and ras-F[3] (III); raf-F[1,2] and zip-F[3] (IV), and zip-F[1,2] and ras-F[3] (V). (*B*) FKBP and TOR2. Cotransformation with FKBP-F[1,2] alone (I); TOR2-F[3] alone (II); FKBP-F[1,2] and TOR2-F[3] (III); vector alone (IV); zip-F[1,2] and TOR2-F[3] (V). (*C*) As in *B*, in the presence of 1 μM rapamycin.

Overexpression of the mutants Z-F[3:Ile-114 → X] was in the same range as Z-F[3], as determined by Coomassie-stained SDS/PAGE (data not shown).

To compare the relative efficiency of reassembly of mutant mDHFR fragments into active enzyme, we measured the bacterial-doubling time in minimal medium. Doubling time under nonselective conditions was essentially constant for all transformants (Table 1). Doubling times under selective conditions (+IPTG and trimethoprim) for cells expressing Z-F[1,2] + Z-F[3], Z-F[1,2] + Z-F[3:Ile-114 → Val], or Z-F[1,2] + Z-F[3:Ile-114 → Ala] were 1.6-fold, 1.9-fold, and 4.1-fold higher, respectively, than the doubling time of *E. coli* expressing full-length mDHFR. No growth was observed for cells expressing Z-F[1,2] + Z-F[3:Ile-114 → Gly]. Cell growth was observed in the absence of induction only with the full-length mDHFR due to low level expression, whereas IPTG induction of full-length mDHFR unexpectedly prevented cell growth. Growth was partially restored by addition of the folate metabolism end-products thymine, adenine, pantothenate, glycine, and methionine (data not shown), suggesting that the overexpressed enzyme binds to and depletes the folate pool.

Methotrexate-Resistant Mutants. It could be argued that the "affinity" mutants reduce activity rather than fragment affinity of reassembled DHFR although Ile-114 is distant from the active site. As a further control for understanding the molecular basis for fragment reassembly, we examined other mutants, which have been previously characterized in full-length DHFR. We mutated F[1,2] at each of five positions that significantly increase K_i (MTX): Gly-15 → Trp, Leu-22 → Phe, Leu-22 → Arg, Phe-31 → Ser, and Phe-34 → Ser. These

Table 1. Relative doubling times of *E. coli* with mutations in liquid media

	No additions	+trimethoprim	+trimethoprim + IPTG
Wild-type mDHFR	1.1 ± 0.2*	1.0 ± 0.2	ng†
zip-[1,2] + zip[3]	1.0 ± 0.2	ng	1.7 ± 0.2
Destabilizing mutations			
zip-[1,2] + zip[3:Ile114Val]	1.0 ± 0.2	ng	2.1 + 0.2
zip-[1,2] + zip[3:Ile114Ala]	1.1 ± 0.2	ng	4.3 ± 0.3
zip-[1,2] + zip[3:Ile114Gly]	1.1 ± 0.2	ng	ng
Methotrexate-resistant mutations‡			
zip-[1,2:Leu22Phe] + zip[3]	1.2	nd	1.6
zip-[1,2:Leu22Arg] + zip[3]	0.85	nd	1.6
zip-[1,2:Phe31Ser] + zip[3]	1.0	nd	1.3

*The OD_{600} at each time point for triplicate samples was plotted to calculate doubling time (according to log A2/A1 = k(T2 − T1), where A = OD_{600} and k = growth constant). The average of two separate experiments is given. Where indicated, trimethoprim was present at 1 μg/ml and IPTG at 1 mM.
†ng, no growth was observed; nd, not determined.
‡Data from a single experiment (triplicate samples).

mutations occur at different positions in space relative to the active site and to F[3] (Fig. 2*B*) and have different effects on K_m (DHF), K_m (NADPH), and V_{max} of the full-length DHFR (21, 22). Overexpression and solubility of all mutants was in the same range as Z-F[1,2], as determined by Coomassie-stained SDS/PAGE (data not shown) with the exception of Z-F[1,2: Phe-34 → Ser], which is less soluble (results not shown). Mutants Z-F[1,2:Leu-22 → Phe], Z-F[1,2:Leu-22 → Arg], and Z-F[1,2: Phe-31 → Ser] all allowed for bacterial growth with high growth rates when cotransformed with Z-F[3] (Table 1). Mutants Z-F[1,2:Gly-15 → Trp] and Z-F[1,2:Phe-34 → Ser] did not allow for bacterial growth. The position of Gly-15 readily explains this observation: it occurs at the interface in a loop that shares many interactions with F[3] and thus probably prevents normal folding and/or fragment affinity in the same way as the Ile-114 mutations do.

Steady–State Kinetic Parameters of the Reconstituted Enzyme. To assess the kinetic effects of fragmentation on DHFR activity, we determined the steady–state kinetic parameters of the purified, reconstituted Phe-31 → Ser mutant. In addition to allowing the evaluation of maintenance of MTX resistance in the reassembled enzyme, the Phe-31 → Ser mutation has the advantage of not being susceptible to the substrate inhibition (by DHF) seen in the wild-type enzyme (23). Binding of DHF and its competitive inhibitor MTX were first investigated. Direct determination of K_m (DHF) at 25 μM NADPH shows that it is in the same range as the full-length mDHFR(Phe-31 → Ser) assayed under similar conditions (21). This NADPH concentration is not saturating (as determined in this study; see Table 2); however, the high quenching by NADPH precluded measurements at saturating NADPH concentrations. Dixon plots of activity in the presence of increasing MTX concentrations, at various fixed DHF concentrations, were generated to determine K_i (MTX) in a manner independent of the DHF concentrations used. K_i (MTX) is in the same range as the full-length mDHFR (Phe-31 → Ser) (Table 2). The K_i was not significantly affected by a 2-fold change in NADPH concentration (data not shown). As the Dixon plots showed MTX to be a true competitive inhibitor of the enzyme, V_{max} was directly determined from the Dixon plots. From this value, k_{cat} (substrate turnover rate) was estimated to be in the range of 6 s^{-1} compared with 5.5 s^{-1} for mDHFR(Phe-31 → Ser). Preliminary direct determination of K_m (NADPH) resulted in a minimum estimate of 20 μM; fluorescence quenching by NADPH precluded a more precise direct measurement. Therefore K_m (NADPH) was determined from Dixon plots of MTX inhibition of DHF binding, at various NADPH concentrations. The V_{max}(apparent) at each NADPH concentration could thus be precisely determined, allowing a replot of V_{max}(apparent) vs. [NADPH]. K_m (NADPH) is ≈3.5-fold higher than that of mDHFR(Phe-31 → Ser) (Table 2). No DHFR activity was detected in untransformed bacteria treated exactly as were bacteria expressing reassembled enzyme.

Induced Hetero-Oligomerization Directed Assembly. We tested the ability of hetero-oligomerizing proteins to assist DHFR reassembly as a further illustration that complementation is general and to illustrate how the strategy can be used to detect protein–protein interactions. We studied the interactions of p21 ras GTPase with its target RBD and of the rapamycin-mediated interaction of the immunophillin FKBP with the yeast TOR2. In both cases, structures of the complexes are known, and as an added restriction, the interaction between the latter is mediated by another molecule providing a further control on oligomerization requirement for DHFR fragment assembly (24, 25). In both cases, cell survival occurred only when complementary DHFR fragments fused to interacting proteins were expressed simultaneously and in the case of FKBP-TOR, only in the presence of effective concentrations of rapamycin (Fig. 4). Lack of observed growth when the protein-DHFR fragment fusions were coexpressed with complementary leucine zipper-DHFR fragments further illustrates the absolute requirement of oligomerization domain-assisted assembly of DHFR.

DISCUSSION

We have demonstrated that the fusion of mDHFR fragments to dimerizing proteins allows for the spatially directed, binary association of the DHFR fragments, promoted by the oligomerization-assistance of the dimerizing proteins. Detection of activity, both *in vivo* and *in vitro*, suggests that native-like folding of the fragments is promoted by their directed association.

We have shown that the rigidity imposed by the covalent linkage between residues 107 and 108 of mDHFR can be replaced by noncovalent leucine zipper interaction resulting in kinetic characteristics similar to full-length enzyme. In a similar way, cleavage of mDHFR at this loop and fusion of the

Table 2. Kinetic parameters determined for the reassembled mDHFR

	K_m(NADPH), μM	K_m (DHF), μM	k_{cat}, s^{-1}	K_i (MTX), nM
Reassembled mDHFR (Phe-31 → Ser)	110	11.1 ± 0.4*	3.2 ± 1.9	0.54 ± 0.33
Full-length mDHFR (Phe-31 → Ser) (ref. 21)	33	4.5	5.5	4.4

*Values given as the mean ± SD for the results of two to five experiments.

native termini has produced a circularly permuted protein with physical and kinetic properties similar to the native enzyme, illustrating that radical modifications in this loop are not disruptive to activity (18). Further, a detailed analysis of prokaryotic and eukaryotic DHFR structures has suggested that loop and subdomain movements are required for catalysis (26). In eukaryotic DHFRs, a loop in residues 59–70 moves to stabilize interactions of DHFR with a transition state analogue. That F[1,2] contains this region intact and the enzyme functions is consistent with this study. Further dissection of F[1,2] into the catalytic loop and nucleotide-binding domain will aid in accessing the importance of this and other loop and secondary structure elements to catalysis.

Protein domain affinity can be reduced by 1–5 kcal/mol by changing the side chain volume in the hydrophobic core of a protein (20).We have illustrated with the fragment interface mutations (Ile-114 and Gly-15) that with an *in vivo* assay we can detect and differentiate mutations that decrease fragment affinity to different degrees. By the same token, the Gly-15 → Trp mutation is tolerated in the full-length DHFR but does not allow complementation. This result suggests that the folding and reassembly of DHFR from fragments is different from that of the full-length enzyme. The three methotrexate-resistant mutants (Leu-22 → Phe, Leu-22 → Arg, and Phe-31 → Ser) centered in the substrate-binding pocket of F[1,2] have effects consistent with characteristics in the full-length enzyme. The mutations are well tolerated and allow for very efficient fragment complementation even though they alter the kinetic parameters of the full-length enzyme relative to the wild-type. This demonstrates that mutations far from the interface can allow productive fragment association; further, we have illustrated the possibility of incorporating desirable characteristics (in this example, methotrexate resistance) into the reassembled enzyme. Phe-34 → Ser does not allow reconstitution of activity. This may be a result of its lower solubility, or of the 5,000-fold reduction in catalytic efficiency relative to the wild-type (22). This position is conserved in 35 of 37 natural sequences (HSSP database file:1drf.hssp) (27) and is part of a hydrophobic cluster in F[1,2]; it may be necessary for the proper folding or stability of this fragment.

Oligomerization domain-assisted fragment reassembly could provide a powerful strategy for enzyme dissection studies in general. The control over the assembly of separate functional domains of enzymes would permit rigorous enzymatic structure/function studies, the definition of structural motifs, and an understanding of their role in catalysis. Detailed knowledge of the enzyme mechanism could be exploited through the combination of different functional "building blocks" with the functional motifs responsible for substrate binding and catalysis in other enzymes, allowing the generation of novel protein catalysts. The possibility of altering an enzyme's catalytic reaction by the combination of a substrate-binding domain and an active site from different enzymes has been demonstrated recently (28); oligomerization domain-assisted assembly offers an efficient strategy for multiple combinations of domains of interest and allows for *in vivo* high-throughput screening as well as *in vitro* characterization of products as in a directed evolution strategy (29, 30).

There is an interesting symmetry to the system described here: the fact that the oligomerization domains are absolutely required for reconstitution means that the reconstitution of activity itself is a detector of the oligomerization domain interactions. Thus the system we describe here can be applied to studying protein–protein interactions *in vivo* in a similar way as other techniques such as the yeast two-hybrid system or other fragment complementation strategies (10–12, 31). We envisage that this application of a protein-fragment complementation assay (PCA) would have certain advantages over other approaches. Principal advantages include the fact that first, no other host-specific processes or enzymes are needed. It thus would be possible to perform selection in any cell type. We are presently pursuing variants of the DHFR PCA in yeast and mammalian cell lines (I. Remy, S.W.M., unpublished data). Secondly, the fact that the structure of the enzyme is known means that it is possible to control the way that interactions can occur. For example, to control for orientation of specifically interacting proteins by fusing them to either N or C termini of the enzyme fragments, one could discriminate between "parallel" vs. "antiparallel" interactions. Finally, the PCA strategy allows for designing a detector of variable stringency by introducing mutations that disrupt fragment complementation. We are currently pursuing the PCA strategy for stringent selection of interacting protein partners from designed libraries (J.N.P., K. Arndt, A. Plückthun, and S.W.M., unpublished data). In a more generalized application, the PCA could be used in screening cDNA libraries for proteins that interact with a known "bait." The simplicity of the *in vivo* assay would ensure that a large number of unknowns could easily be screened for interactions.

This work was supported by the Medical Research Council of Canada (Grant DGN 095) and by the Burroughs-Wellcome Fund (S.W.M.). J.N.P. is a recipient of a fellowship from Les Fonds pour la recherche en santé du Québec. S.W.M. is an awardee of a Burroughs-Wellcome Fund New Investigator Award in the Basic Pharmacological Sciences. Tetrahydrofolate was generously donated by Robert MacKenzie (McGill University). We are grateful to Monique Davis for the pMT3 vectors, Joe Heitman for pMRS315, Emil Pai for ptcras, David Waugh for pDW333, and Stuart L. Schreiber for pNH1.

1. Ullmann, A., Jacob, F. & Monod, J. (1967) *J. Mol. Biol.* **24,** 339–343.
2. Taniuchi, H. & Anfinsen, C. B. (1971) *J. Biol. Chem.* **246,** 2291–2301.
3. Ladurner, A. G., Itzhaki, L. S., Gay, G. D. & Fersht, A. R. (1997) *J. Mol. Biol.* **273,** 317–329.
4. de Prat Gay, G., Ruiz-Sanz, J. & Fersht, A. R. (1994) *Biochemistry* **33,** 7964–7970.
5. Shiba, K. & Schimmel, P. (1992) *Proc. Natl. Acad. Sci. USA* **89,** 1880–1884.
6. Tasayco, M. L. & Carey, J. (1992) *Science* **255,** 594–597.
7. Bertolaet, B. L. & Knowles, J. R. (1995) *Biochemistry* **34,** 5736–5743.
8. Michaels, J. E., Schimmel, P., Shiba, K. & Miller, W. T. (1996) *Proc. Natl. Acad. Sci. USA* **93,** 14452–14455.
9. Pelletier, J. N., Remy, I. & Michnick, S. W. (1998) *J. Biomol. Tech,* in press.
10. Johnsson, N. & Varshavsky, A. (1994) *Proc. Natl. Acad. Sci. USA* **91,** 10340–10344.
11. Rossi, F., Charlton, C. A. & Blau, H. M. (1997) *Proc. Natl. Acad. Sci. USA* **94,** 8405–8410.
12. Karimova, G., Pidoux, J., Ullmann, A. & Ladant, D. (1998) *Proc. Natl. Acad. Sci. USA* **95,** 5752–5756.
13. Gegg, C. V., Bowers, K. E. & Matthews, C. R. (1997) *Protein Sci.* **6,** 1885–1892.
14. Bystroff, C. & Kraut, J. (1991) *Biochemistry* **30,** 2227–2239.
15. Oefner, C., D'Arcy, A. & Winkler, F. K. (1988) *Eur. J. Biochem.* **174,** 377–385.
16. Protasova, N., Kireeva, M. L., Murzina, N. V., Murzin, A. G., Uversky, V. N., Gryaznova, O. I. & Gudkov, A. T. (1994) *Protein Eng.* **7,** 1373–1377.
17. Kaufman, R. J., Davies, M. V., Pathak, V. K. & Hershey, J. W. (1989) *Mol. Cell. Biol.* **9,** 946–958.
18. Buchwalder, A., Szadkowski, H. & Kirschner, K. (1992) *Biochemistry* **31,** 1621–1630.
19. Appleman, J. R., Prendergast, N., Delcamp, T. J., Freisheim, J. H. & Blakley, R. L. (1988) *J. Biol. Chem.* **263,** 10304–10313.
20. Chen, X., Rambo, R. & Matthews, C. R. (1992) *Biochemistry* **31,** 2219–2223.
21. Thillet, J., Absil, J., Stone, S. R. & Pictet, R. (1988) *J. Biol. Chem.* **263,** 12500–12508.
22. Nakano, T., Spencer, H. T., Appleman, J. R. & Blakley, R. L. (1994) *Biochemistry* **33,** 9945–9952.
23. Chunduru, S. K., Cody, V., Luft, J. R., Pangborn, W., Appleman, J. R. & Blakley, R. L. (1994) *J. Biol. Chem.* **269,** 9547–9555.
24. Choi, J., Chen, J., Schreiber, S. L. & Clardy, J. (1996) *Science* **273,** 239–242.
25. Nassar, N., Horn, G., Herrmann, C., Scherer, A., McCormick, F. & Wittinghofer, A. (1995) *Nature (London)* **375,** 554–560.
26. Sawaya, M. R. & Kraut, J. (1997) *Biochemistry* **36,** 586–603.
27. Sander, C. & Schneider, R. (1991) *Proteins* **9,** 56–68.
28. Nixon, A. E., Warren, M. S. & Benkovic, S. J. (1997) *Proc. Natl. Acad. Sci. USA* **94,** 1069–1073.
29. Kuchner, O. & Arnold, F. H. (1997) *Trends Biotechnol.* **15,** 523–530.
30. Crameri, A., Dawes, G., Rodriguez, E., Silver, S. & Stemmer, W. (1997) *Nat. Biotechnol.* **15,** 436–438.
31. Fields, S. & Song, O. (1989) *Nature (London)* **340,** 245–246.
32. Cody, V., Luft, J. R., Ciszak, E., Kalman, T. I. & Freisheim, J. H. (1992) *Anti-Cancer Drug Des.* **7,** 483–491.